Oxide Inclusions and Tool Wear in Machining

GLORIA M. FAULRING AND S. RAMALINGAM

The inclusions formed in experimental steels by calcium, aluminum, and silicon additions are characterized. The morphology, phase identity, elemental analyses, and semiquantitative wt pct of the inclusions in each steel are presented. A correlation of tool wear tests conducted on the experimental steels and the inclusion characteristics indicates that a major factor in tool flank wear is the high temperature hardness of the inclusion phases or inclusion abrasion. A steel containing glass-like inclusions produced minimal tool wear but when the inclusions were a crystalline silicate, tool wear increased. The most severe tool wear occurred when machining steels with $CaO \cdot 6Al_2O_3$, Al_2O_3, and/or AlN as the major inclusion phases. By judicious selection of the deoxidation practice, the formation of refractory type oxide inclusions may be prevented and inclusions that enhance machinability may be formed.

THE relationship between the metallurgy of iron-base alloys and machinability is complex. The influence of deoxidation practice on tool wear is generally accepted but there are conflicting views on the wear mechanism. Theories of diffusion and attrition by abrasive wear have been advanced to account for tool wear. Both are related to the quantity and characteristics of the inclusions as well as the effect of temperature on their hardness and deformability.

In this study, the inclusions formed by calcium, aluminum, and silicon deoxidants were characterized. The morphology, phase identity, elemental analyses, and semiquantitative wt pct of the inclusions were determined. From a correlation of the tool wear tests conducted on the experimental steels and the collected data, it was concluded that tool wear is greatly influenced by the abrasive properties of the inclusions in the steel.

MATERIALS DESCRIPTION

The experimental 1040 grade laboratory steels examined in this investigation were made by melting Swedish iron with controlled additives. The series of steels labeled V was vacuum melted and the ones designated L, air melted. Both series were cast into preheated cast iron molds 4 in. (10.2 cm) thick, reheated to 1180 to 1200°C., held at this temperature for four h, and then hot rolled at 1150 to 1180°C. After rolling, the temperature was approximately 1100°C. From 121 lb (55 kg) billets, the V series was rolled to 1.625 in. (4.1 cm) diam and the L series to 2.75 in.^{2} (7 cm^2).

The steels were cooled to room temperature in still air following hot rolling. As was expected, the structure was intermediate between normalized and annealed 1040 grade steel. Visual examination showed the microstructures of both series of steels were similar and consisted of nearly equal amounts of pearlite and ferrite with no ferrite network around the pearlite. The structure was typical of annealed steels.

GLORIA M. FAULRING, formerly Graduate Student, State University of N.Y. at Buffalo, is now with Union Carbide Corporation, Metals Division, Niagara Falls, NY 14302. S. RAMALINGAM, School of Mechanical Engineering, Georgia Institute of Technology, Atlanta, GA 30332.

Manuscript submitted December 28, 1978.

Chemical analyses of randomly selected samples of each heat showed that the compositions of the two series of steels were within the ranges listed below.

Melt Series	Pct C	Pct Mn	Pct P	Pct Si
V	0.38-0.42	0.71-0.79	0.015-0.017	0.24-0.31
L	0.37-0.40	0.70-0.74	0.012-0.014	0.20-0.31

The calcium, sulfur, and aluminum analyses and deoxidant added to each heat are listed in Table I. When the aluminum and sulfur contents were less than 10 ppm, they could not be measured accurately by optical spectrographic methods. However, the calcium determinations have a precision of about ±2 ppm. These analyses were made by an atomic absorption-spectrophotometric method designed for the determination of calcium in steel.[1]

INCLUSION CHARACTERIZATION

Polished specimens of each of the steels were examined optically. Next, they were etched electrolytically* and examined on a scanning electron microscope (SEM). Although this etching procedure attacks sulfides, it was not a deterrent in this investigation because the major objective was oxide inclusion characterization. The SEM images in Figs. 1 to 3, 4(*a*) and (*b*) are typical of the inclusions in the polished-etched specimens; and in Fig. 4(*c*), optical images of a polished specimen. Since the SEM was equipped for elemental analyses, the inclusions were also analyzed. The results are discussed below.

*Perchloric acid (60 pct conc.-8 vol pct), water (12 vol pct), glycerol (10 vol pct), and ethanol (95 pct conc.-70 vol pct).

With the exception of V1629, only aluminum was detected in the oxide inclusions in the vacuum melted steels. As shown in Fig. 1, some were angular and others nearly spherical. In addition to alumina, V1629 contained a small to trace amount of calcium aluminate. The oxides in this series were encapsulated in manganese sulfide.

In contrast to the vacuum melted steels, the inclusions in each of the air melted steels were of different compositions. In L64, the inclusions were silicon plus small to trace amounts of aluminum and manganese;

ISSN 0360-2133/79/1112-1781$00.75/0

Table I. Chemical Analyses

Melting Practice	Sample No.	Wt Pct S	Wt Pct Al	Wt Pct Ca	Deoxidant
Vacuum	V1632	0.02	0.054	0.001	Ca-Si
	V1624	0.021	0.045	0.002	Ca-Si
	V1631	0.015	0.082	0.001	Ca-Ba-Al-Si
	V1629	0.03	0.02	0.001	Ca-Si
Air	L64	<0.001	<0.001	0.001	Ca-Si
	L65	0.017	0.047	0.001	Ca-Ba-Al-Si
	L66	0.025	0.004	0.001	Ca-Si

and their shape, elongated and somewhat elliptical, Fig. 2. Small globular sulfides were frequently attached to the surface or occurred as an integral part of the oxide. The high magnification image, Fig. 2(*b*), emphasizes the complex morphology of these inclusions. The oxides in L65, Fig. 3, are typical of calcium-aluminum deoxidized steels containing 20 ppm calcium and 0.05 pct aluminum, *i.e.*, hexagonal symmetry and aluminum rich with a small amount of calcium ($CaO \cdot 6Al_2O_3$). In L66, Fig. 4, the oxides were an aluminum silicate phase containing a small amount of manganese. Since their location around the exterior of the manganese sulfides was unusual, the optical images, Fig. 4(*c*), are included. The top one was taken with reflected ordinary light, and the lower one with reflected polarized light and crossed Nicols, both of the same area. The polarized light image shows that the anisotropic silicate phase (nearly white) is located around the isotropic (dark) central zone of manganese sulfide.

SEMIQUANTITATIVE WEIGHT PERCENTAGES AND PHASE IDENTIFICATION

The quantity of inclusions in a steel is important in the overall influence of inclusions on machinability. The phase identification is also required to correlate tool wear and inclusion properties. In order to obtain

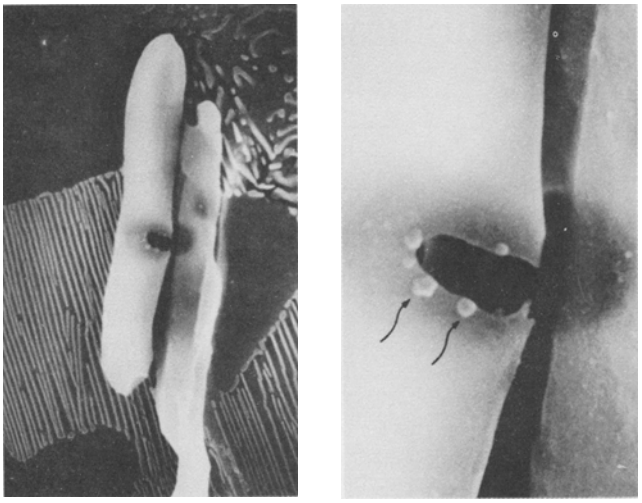

(*a*) (*b*)

Fig. 2–Heat no. L64, Air melted steel (etched): (*a*) magnification 3,480 times, (*b*) magnification 17,400 times.

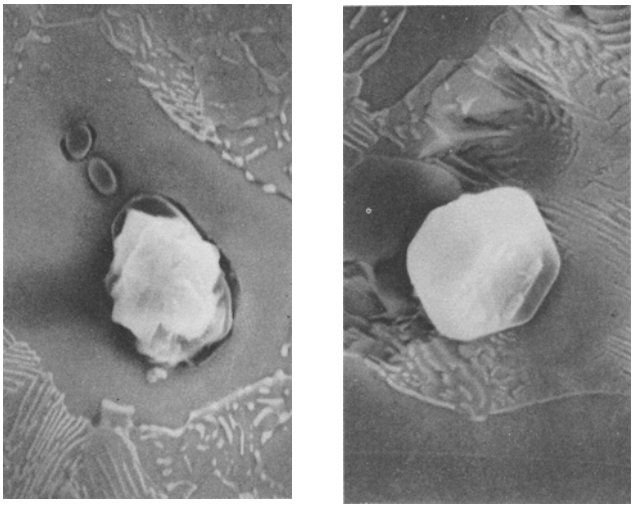

(*a*) (*b*)

Fig. 3–Heat no. L65, Air melted steel (etched): (*a*) magnification 4,350 times, (*b*) magnification 4,350 times.

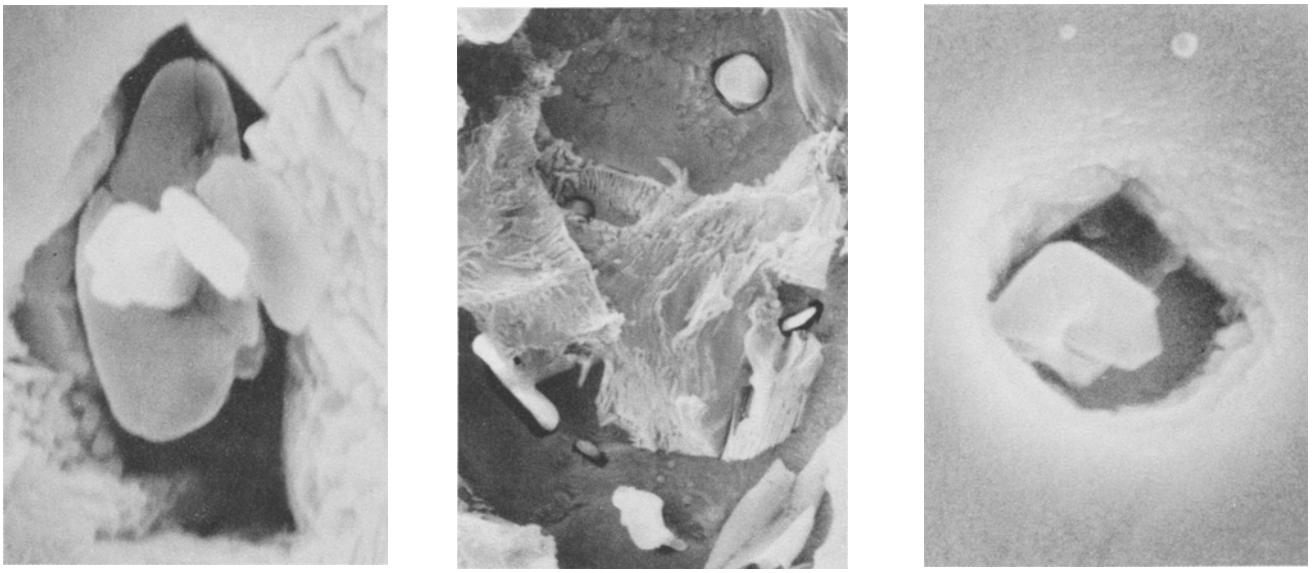

(*a*) (*b*) (*c*)

Fig. 1–Vacuum melted steels (etched): (*a*) Heat no. V1624 magnification, 10,000 times, (*b*) Heat no. V1629 magnification, 2,000 times, and (*c*) Heat no. V1632 magnification, 10,000 times.

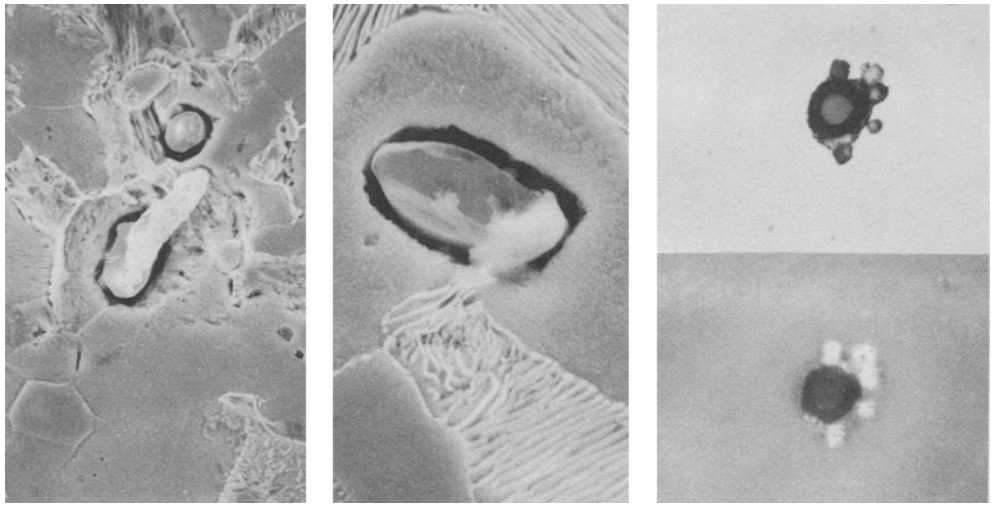

(a) (b) (c)

Fig. 4—Heat no. L66, Air melted steel: (*a*) and (*b*) SEM images of etched specimen, and (*c*) optical images of polished specimen. Upper one taken with ordinary light and lower one with polarized light and cross Nicols: (*a*) magnification 2000 times, (*b*) magnification 5000 times, and (*c*) magnification 1500 times.

these data, the inclusions were extracted and examined on the scanning electron microscope and by X-ray diffraction. Some of the inclusions were also analyzed by optical spectroscopy and with an electron microprobe to identify trace elements.

Weighed amounts of each of the steels were dissolved in various solvents and the wt pct of the insoluble residues determined. Primarily, aqueous nitric acid or bromine-methanol solutions were used as solvents. Some of the extracted residues from the nitric acid treatment were followed by leaching with a very dilute basic solution. Samples were also dissolved in bromine-methyl acetate or electrolytically in a perchloric-acetic acid solution. The inclusion bearing solution was filtered on a preweighed 0.45 μ pore size cellulose ester or Fluorpore* filter with the extraction media determining the filter material selected. The temperature and humidity of the filters were controlled for the initial and final (after filtering) weighing. Each extraction was repeated several times but there was sufficient variations that the data must be considered as semiquantitative. The numerous difficulties encountered in quantitative inclusion analyses have been discussed by Bandi.[2] The results are summarized in Table II.

*Product of Millipore Corporation.

The phases in the extracted residues were analyzed by X-ray diffraction and sections of the filters examined on the scanning electron microscope. In Table III, the phases identified in each sample are listed in order of decreasing amounts. SEM images typical of the various phases are shown in Figs. 5 and 6.

The presence of γ, η, and Δ aluminas in the vacuum melted experimental steels, Table III, shows rapid cooling. These phases occurred as very small, nearly equidimensional particles (Fig. 5). In V1629, there were a few $CaO \cdot 6Al_2O_3$ inclusions. For example, see arrow in Fig. 5(*b*). The AlN phase in V1631 (0.08 pct Al) was detected in the nitric acid extracted residues. Although this is unusual, the occurrence of acid insoluble AlN in high aluminum steels has been previously reported by Piper *et al*.[3]

The diffraction patterns obtained from the colorless residues extracted from L64 were faint or nonexistent; and from L66, distinct, intense and characteristic of mullite ($Al_6Si_2O_{13}$). The inclusions in L64 were isotropic and silicon rich; and in L66, anisotropic and aluminum and silicon rich with a small amount of manganese. The morphology of both was similar but the inclusions in L64 were soluble in dilute NaOH and in L66, insoluble. Compare Fig. 6(*b*) and (*c*). It was concluded that the inclusions in L64 are a glass-like, silica rich phase; and in L66, a mullite type phase with a crystallite size between 0.1 and 10 μ.

The hexagonal symmetry of the inclusions extracted

Table II. Semiquantitative Oxide Inclusion Content of Experimental Steels

		Inclusion Content	
	Sample	Wt Pct	Vol Pct (Calc.)*
Vacuum Melted:	V1632	0.004	0.007
	V1624	0.007	0.014
	V1631	0.003	0.006
	V1629	0.006	0.012
Air Melted:	L64	0.065	0.217
	L65	0.02	0.053
	L66	0.024	0.056

*Densities estimated from identified phases, intensities of X-ray diffraction patterns and optical spectrographic analyses.

Table III. X-ray Diffraction Analyses of Extracted Residues

Vacuum Melted			
Heat No. V1624	Heat No. V1629	Heat No. V1631	Heat No. V1632
α-Al_2O_3	α-Al_2O_3	γ-Al_2O_3	α-Al_2O_3
Δ-Al_2O_3	η-Al_2O_3	AlN	γ-Al_2O_3
	$CaO \cdot 6Al_2O_3$		η-Al_2O_3

Air Melted		
Heat No. L64	Heat No. L65	Heat No. L66
Primarily Amorphous	$CaO \cdot 6Al_2O_3$	$Al_6Si_2O_{13}$(Mullite Type)
SiO_2(Quartz)	AlN	α-Al_2O_3
SiO_2(Cristobalite) Trace Amounts	α-Al_2O_3	SiC(Trace)
SiC		

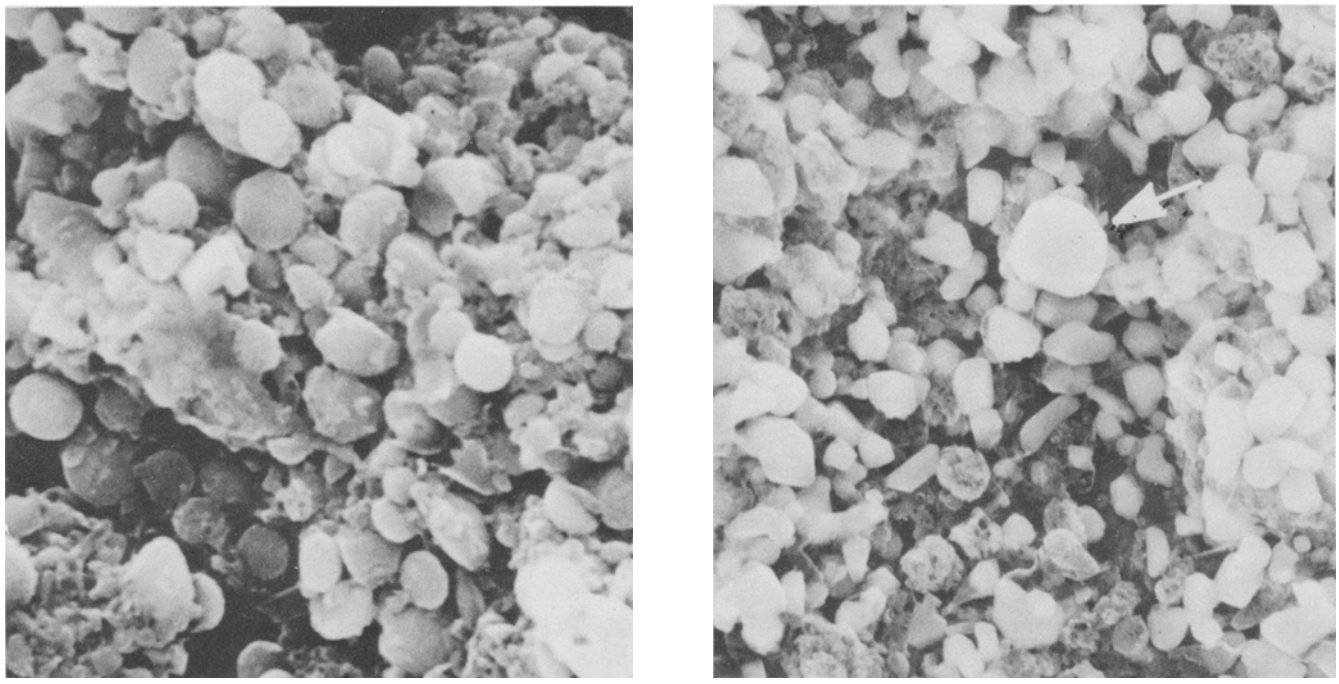

(a) (b)

Fig. 5—Vacuum melted steels. Inclusions extracted in aqueous HNO_3 (20 pct) and then treated with: (*a*) aqueous NaOH(0.1 pct) and (*b*) aqueous Na_2CO_3(6 pct): (*a*) Heat no. V1631, magnification 6,000 times, (*b*) Heat no. V1629, magnification 2,400 times.

from L65 is characteristic of the $CaO \cdot 6Al_2O_3$ phase (Fig. 6(*d*)). In commercial steels, these hexagonal inclusions frequently agglomerate into nearly spherical particles that lack optical anisotropy and have the glass-like appearance observed by other investigators.[1]

DISCUSSION

In steels containing 0.045 to 0.082 pct aluminum, more than 10 to 20 ppm calcium are required to form a calcium aluminate phase under fast cooling conditions. In these steels, the occurrence of γ, η, and Δ Al_2O_3 is evidence of rapid cooling. Thus, steels V1632, V1631, and V1624 were, in effect, aluminum deoxidized and did not contain any calcium aluminate phases.

The oxide inclusions in V1629 were primarily α-Al_2O_3 with small amounts of η-Al_2O_3 and $CaO \cdot 6Al_2O_3$. It may be noted that when a steel contains 0.02 pct aluminum, 10 ppm calcium is enough to produce some $CaO \cdot 6Al_2O_3$. In the other steels of this series, the amount of calcium relative to that of the aluminum was appreciably less. In addition, the angularity of some of the alumina inclusions in V1629 suggests a slower cooling rate. Although V1629 was calcium-aluminum deoxidized, the major effect of the calcium was to modify some of the alumina inclusions, not deoxidize the steel.

In the air melted steels L64 and L66, the elongated, somewhat elliptical shape of the inclusions is a result of the deformation produced during rolling. The silica rich inclusions in L64 indicate silicon deoxidation and the aluminum-silicon rich oxides in L66, aluminum plus silicon deoxidation. Based on the semiquantitative wt pct determinations of inclusions, L64 contains about 2 1/2 times more inclusions by weight and about four times more by volume than L66. Chemical analyses (Table I) show that L64 contains 10 ppm calcium and <0.001 pct aluminum and sulfur; and L66, 10 ppm calcium, 0.004 pct aluminum and 0.025 pct sulfur. The very low aluminum and sulfur contents, <0.001 pct, in L64 were expected since these were laboratory heats made from nearly pure source materials and there was no intentional addition of these elements.

The major inclusion phase in L65, $CaO \cdot 6Al_2O_3$, was hexagonal in shape and 5 μ and less in size. The phases AlN and α-Al_2O_3 were present in only small amounts. The vol and wt pct of the inclusions in the air melted steels L65 and L66 were similar (density of mullite ($Al_6Si_2O_{13}$) = 3.156; of $CaO \cdot 6Al_2O_3$ = 3.38).

Tool Wear

The large differences in machinability for steels having the same compositions are considered by some investigators to be related to variations in steelmaking practice such as time of pouring, leach-out of refractories, ladle time, solidification rate, and so forth.[4] These variations are sufficient to influence the size, shape, and type of inclusions formed and, thus, the machinability.

It has been postulated that the gradual removal of the surface material from a cutting tool during machining is related to the presence of refractory type inclusions.[5] Supportive evidence may be found in the abrasiveness of small particles in fine grain steels. These steels are known for their high tool wear and are produced by adding grain refiners such as niobium (Cb), vanadium, and aluminum in very small amounts (250 to 800 ppm). All of these elements produce refractory type inclusions. In contrast, soft inclusion type materials such as lead are added to steels to decrease tool wear.

A comparison of the high temperature hardness of inclusion type phases, tungsten carbide, titanium car-

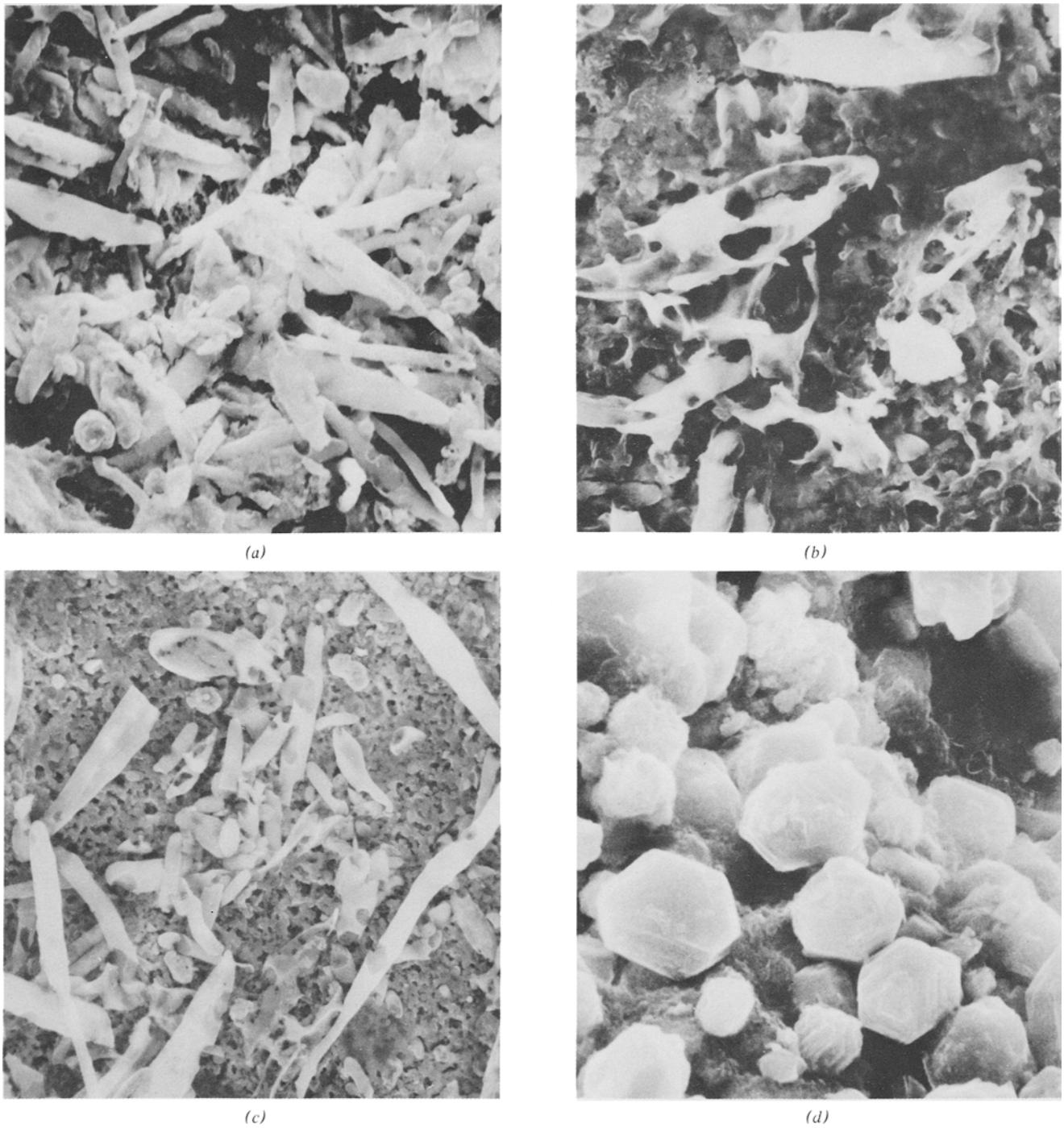

Fig. 6—Air melted steels. Inclusions extracted in aqueous HNO_3 (20 pct): (*a*) As-extracted, (*b*), (*c*), and (*d*) after extraction, treated with aqueous NaOH(0.2 pct): (*a*) Heat no. L64, magnification 1,160 times, (*b*) Heat no. L64, magnification 2,320 times, (*c*) Heat no. L66, magnification 1,160 times, and (*d*) Heat no. L65, magnification 3,480 times.

bide, and high speed steels, also showed the feasibility of abrasive wear.[6] At temperatures prevailing during machining, the hardness of the inclusions exceeds that of the matrix. For example, the major inclusion phase found in the steels examined in the previous section was alumina. Alumina has a Vickers' microhardness of 1,700 kg/mm^2 at 700°C,[7] whereas cementite has a hardness of 98 kg/mm^2; titanium carbide, 500 kg/mm^2; and tungsten carbide (WC), 180 kg/mm^2.[8-11]

In order for the abrasive wear mechanism to be valid, the number of nonmetallic inclusions crossing the surface of the tool must exceed the number of debris particles produced. Ramalingam and Watson[4] calculated that 1) the number of nonmetallic inclusions encountered during machining exceeds the number of wear debris particles by two orders of magnitude, and 2) the occurrence of nonmetallic inclusions in the range of several hundred parts per million (volume) is sufficient to produce wear.

In a recent article, wear was considered as the detachment of small particles from the surface of the tool by a "multitude of injuries" by abrasive particles.[12] In an effort to relate the properties of inclusions to tool wear, tool wear tests were conducted on

the experimental steels previously examined. The results of these tests are represented graphically in Figs. 7 to 9.

The sulfur contents of the experimental steels were not sufficient to produce a measurable effect on the tool wear tests. For example, a correlation of the sulfur contents, Table I, and the tool wear rates listed below shows that steel L64 contained <0.001 pct sulfur and produced a wear rate of 1.3 μ/min, whereas the tool wear rate from machining L66, 0.025 pct sulfur, was 3 μ/min. In addition, the steels had the same microstructures and nearly the same compositions. The major difference was the amounts and identities of the inclusions. Thus, the relationship between the properties and amounts of the refractory type inclusions and tool wear was examined. The results are discussed in the following section.

Cutting Conditions: Carbide tool (12 mm^2, 3.18 mm thick), 0.4 mm nose radius, 11 deg clearance angle, 5 deg rake angle, 15 deg approach angle.

Carbide Tool Designation: ISO Grade P30, Geometry SPUN 304.

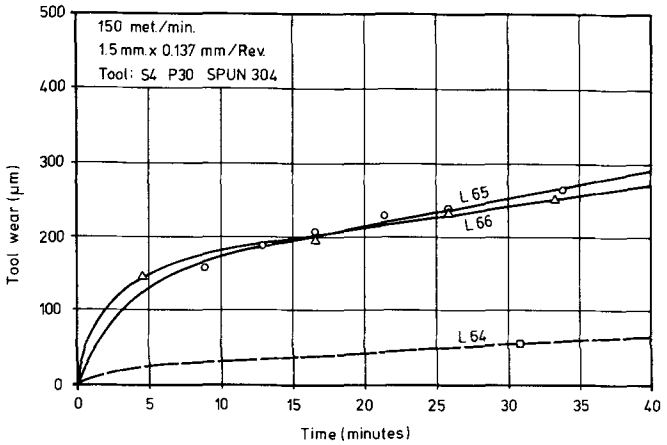

Fig. 7—Flank wear of carbide tools produced during machining air melted steels, heat nos. L64, L65, and L66, with indicated cutting conditions.

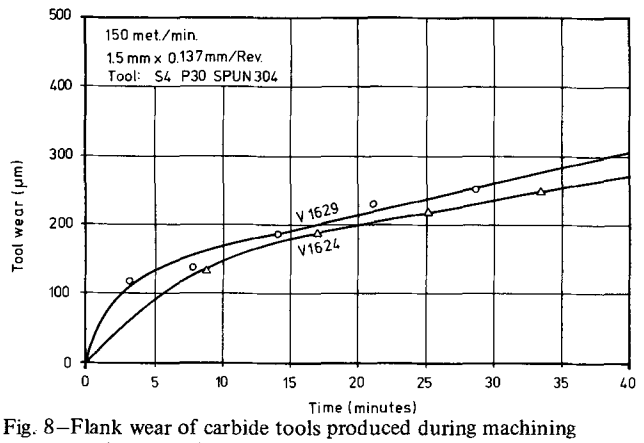

Fig. 8—Flank wear of carbide tools produced during machining vacuum melted experimental steels, heat nos. V1624 and V1629, with indicated cutting conditions.

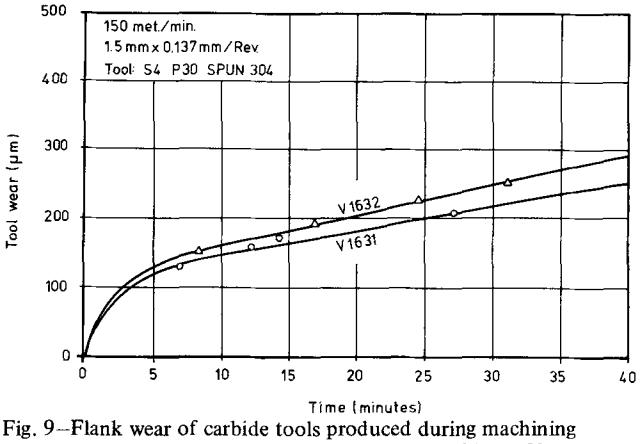

Fig. 9—Flank wear of carbide tools produced during machining vacuum melted experimental steels, heat nos. V1631 and V1632, with indicated cutting conditions.

Vacuum Melted Steels		Air Melted Steels	
No.	Tool Wear Rate, μ/min	No.	Tool Wear Rate, μ/min
V1624	3.4	L64	1.3
V1629	4.8	L65	3.8
V1631	3.2	L66	3.0
V1632	4.3		

Air Melted Experimental Steels

Based on the chemistry (0.2 pct Si and 0.75 pct Mn), melting in air and a relatively large inclusion volume of 0.22 pct, one would expect L64 to produce a high tool wear rate. However, the observed wear rate was exceptionally low, *i.e.*, 1.3 μ/min. The inclusions were a silica rich, glass-like phase that had elongated but not crystallized during rolling. In addition, they probably remained in a glassy state that softened during machining. As a result, the hardness of the inclusions when traversing the tool surface was appreciably less than that of the tool and any abrasion and flow restraint on the tool surface was diminished. Not only did the formation of these inclusions enhance machinability by decreasing tool wear, they also formed instead of refractory type oxides during solidification. Thus, by judiciously choosing the deoxidant, the detrimental effect of inclusions on tool wear can be eliminated or, as in this case, be beneficial. In a recent discussion of machinability enhancement, inclusion properties that should decrease tool wear were postulated by Ramalingam,[5] The inclusions in L64 support the hypothesis advanced.

The tool wear rate produced on machining L66 was about 2 1/2 times greater than that of L64, Fig. 7. Steel L66 contained 0.20 pct silicon, 0.004 pct aluminum, and 10 ppm calcium; and L64, 0.27 pct silicon, <0.001 pct aluminum, and 10 ppm calcium. The shape and size of the inclusions in both were similar but the inclusions in L66 were a mullite type phase with a crystallite size of 0.1 to 10 μ and in L64, a glass-like phase. The probable as-cast shape and subsequent deformability during rolling suggest that the solidification rate was rapid enough to retain the inclusions in both steels in a metastable condition in the as-cast ingot. The combination of reheating and deformation during rolling was sufficient to transform the amorphous inclusions in L66 to a crystalline phase but not in L64. The differences in wear rate produced by these steels may be explained by examining the hardness of these inclusion phases.

Mullite is nondeformable, at least up to a temperature of 1000°C. At room temperature, the hardness of

mullite resembles that of α-quartz. Kiessling[13] reports that the microhardness of mullite is 1500 kp/mm^2 and of α-quartz, about 1600 kp/mm^2. At elevated temperatures, quartz maintains a high level of hardness.[7] Since the crystal structure of mullite consists of strings of silica tetrahedra and microhardness is related to bond strength, mullite may also have a high hardness at elevated temperatures.

Based on only the crystallinity of the mullite phase, it may be reasonably assumed that the hardness of the mullite type inclusion phase in L66 is greater than that of the glass-like inclusions in L64. In addition, the tool wear tests indicated that 0.06 vol pct of mullite type inclusions was sufficient to abrade the carbide tool at a greater rate than 0.22 vol pct of glass-like inclusions. The wear rate produced by the mullite type inclusions, however, was not as great as that of the alumina bearing steels. This agrees with the hardness values measured at room temperatures, *i.e.*, mullite ($Al_6Si_2O_{13}$) < $CaO \cdot 6Al_2O_3$ < α-Al_2O_3. Compare Figs. 7 to 9.

The tool wear rate by steel L65, 0.047 pct aluminum, and 10 ppm calcium, was the highest of the air melted steels (3.8 μ/min). The inclusions were primarily $CaO \cdot 6Al_2O_3$ and small amounts of α-Al_2O_3 and AlN. Alumina has a Vickers' microhardness of 800 kg/mm^2 at 700°C and ≥650 kg/mm^2 at 800°C.[9] The aluminum to oxygen bonding in $CaO \cdot 6Al_2O_3$ should be similar to that of α-Al_2O_3. Kiessling[13] established that the hardness of the calcium aluminates increases with the alumina content; and that the microhardness of $CaO \cdot 6Al_2O_3$ is 2200 kp/mm^2 and of α-Al_2O_3, 3000 to 4500 kp/mm^2. Thus, at elevated temperatures, $CaO \cdot 6Al_2O_3$ is probably hard but not as hard as α-Al_2O_3. Rundle[14] reported that AlN has a high melting point and proposed that the bonds between the aluminum and nitrogen atoms are strong, directional, and covalent. Thus, AlN should also be hard at elevated temperatures.

Based on differences in solubility in the various extraction media, approximately one-third of the inclusions in L65, 0.02 wt pct, were $CaO \cdot 6Al_2O_3$ and α-Al_2O_3. These two phases represented about 0.007 wt pct. The remaining 0.013 wt pct was primarily AlN and a small amount of unidentified oxides. Although the high temperature hardness of these phases has not been determined, the tool wear data suggest that an abrasive wear mechanism can account for the observed wear rates.

Vacuum-Melted Experimental Steels

The flank wear produced by V1629 was greater than that of V1624 (Fig. 8), however, both steels contained α-Al_2O_3 as the major inclusion phase and the inclusion contents were nearly the same (Table IV). Similar observations may be made for V1632 and V1631, Fig. 9. As shown in Table IV, these steels also contained about the same amounts of inclusions but V1632 produced greater wear than V1631. In an investigation on the effect of abrasive particles, Byrd and Ferguson[15] reported an increase in tool flank wear with particle size. Assuming the largest particles observed in each steel are a measure of the relative inclusion size, the particle sizes listed in Table IV were assigned to each steel, *i.e.*, V1629, 8 μ; V1624, 5 μ; V1632, 2.7 μ; V1631, 1.5 μ. Thus, the relative wear rates of V1629 and V1632 and of V1632 and V1631 are consistent with the data of Byrd and Ferguson, but the similarity in wear rates of V1632 and V1624 and of V1632 and V1629 cannot be explained on the basis of particle size. Thus, particle size is a factor but the amount, number of particles *vs* size, and identity or high temperature abrasiveness of the inclusion phases must also be considered.

Table IV. Summary of Inclusion Data–Vacuum Melted Steels

Steel	Inclusion Data: Phases	Wt Pct, ppm	Vol Pct, ppm	Size*, μ	Wear Rate, μ/min
V1629	α-Al_2O_3, η-Al_2O_3, C·6A†	60	120	8	4.8
V1624	α-Al_2O_3, Δ-Al_2O_3	70	140	5	3.4
V1632	α-Al_2O_3, γ-Al_2O_3, η-Al_2O_3	40	70	2.7	4.3
V1631	α-Al_2O_3, AlN	30	60	1.5	3.2

*Maximum observed size.
†C·6A–$CaO \cdot 6Al_2O_3$.

SUMMARY

The oxide inclusions in aluminum, calcium-aluminum, and calcium-silicon deoxidized, vacuum and air melted experimental steels were characterized. The morphology, phase identity, elemental analyses and semiquantitative wt pct were determined. The flank wear rates of the tools used in machining these steels were correlated with the properties of the inclusions. The results were as follows:

1. The tool wear rate produced during machining a steel containing glass-like inclusions was extremely low, but when a steel containing mullite type inclusions was machined, the tool wear increased appreciably. The glass-like and mullite type inclusions were similar in size and shape.
2. The wear rate of tools by vacuum and air melted steels deoxidized with aluminum and, in some cases, aluminum and calcium was greater than that of the air melted steels which were, in effect, deoxidized with silicon and silicon plus aluminum.
3. The high tool wear rates observed when machining steels containing mixtures of $CaO \cdot 6Al_2O_3$, AlN, and/or various alumina phases may be accounted for by the high temperature hardness of these inclusion phases.

CONCLUSIONS

Tool wear tests on a steel containing glass-like inclusions showed an extremely low tool wear rate. The inclusions had a low softening temperature and no tendency to crystallize. The properties of these inclusions and the low wear rate are in agreement with the characteristics as necessary to decrease tool wear.

Although the high temperature hardness of many of the inclusion phases is not known, the data collected suggest that abrasion is the most probable wear mechanism. This conclusion is based on the trend in wear rates and inclusion identities tabulated below.

Increase in High Temperature Hardness ↓	Inclusion Identification	Tool Wear Rate, μ/min
	Glass	1.3
	Mullite type	3.0
	$CaO \cdot 6Al_2O_3$ } Aluminas and AlN }	3.2-4.8

ACKNOWLEDGMENT

The experimental melts used in this study were made in the BHP laboratories. We acknowledge the support and interest in this work of Drs. W. J. M. Tegart, G. Brown and J. D. Watson, BHP Melbourne Research Laboratory, Clayton, Victoria, Australia. Particular thanks are accorded Mr. Howard Sheehe of the State University of New York at Buffalo who was unstinting in his cooperation with us. The results reported here are also a derivative of the work funded by the N.S.F. Grant No. 75-09876.

REFERENCES

1. D. C. Hilty and J. W. Farrell: *Iron Steelmaker,* 1975, vol. 2, no. 5, pp. 17-22; no. 6, pp. 20-27.
2. W. R. Bandi: *Science,* 1977, vol. 196, no. 4286, pp. 136-42.
3. E. Piper, H. Hadedorn, H. Kern, and J. Ingeln: *Radex-Rundsch.,* 1957, vol. 5-6, pp. 727-31.
4. S. Ramalingam and J. D. Watson: *1977 Manufacturing Engineering Transactions; Fifth North American Metalworking Research Conference Proceedings,* vol. 5, pp. 291-96, University of Mass., Amherst, Mass., 1977.
5. S. Ramalingam: *J. Eng. Ind.,* 1978, vol. 100, no. 2, pp. 201-09.
6. S. Ramalingam: *Mater. Sci. Eng.,* 1977, vol. 29, no. 2, pp. 123-29.
7. J. H. Westbrook: *Rev. Hautes Temp. et Refract.,* 1966, vol. 3, no. 1, pp. 47-57.
8. K. B. Gove and J. A. Charles: *Met. Technol.,* 1974, vol. 1, pt. 6, pp. 279-83.
9. A. G. Atkins, C. A. Brookes, and M. J. Murray: *Rev. Hautes Temp. Refract.,* 1966, vol. 3, no. 1, pp. 19-25.
10. D. Tabor: *Materials for Metal Cutting,* pp. 21-24, ISI Publ. no. 126, The Iron and Steel Inst., London, 1970.
11. G. V. Samsonov, M. S. Kovalchenko, V. V. Dzmelinskii, and G. S. Upadyaya: *Phys. Status Solidi (a),* 1970, vol. 1, pp. 327-31.
12. S. Ramalingam: *J. Eng. Ind.,* 1977, vol. 99, no. 3, pp. 523-31.
13. R. Kiessling: ISI Spec. Report No. 90, vols. 1 to 3, 1964.
14. R. E. Rundle: *Acta Crystallogr.,* 1948, vol. 1, pp. 180-87.
15. J. D. Byrd and B. L. Ferguson: *1978 Manufacturing Engineering Transactions; Sixth North American Metalworking Research Conference Proceedings,* vol. 6, pp. 310-16, University of Florida, Gainesville, Fla., 1978.